Fuel 327 (2022) 124973

Contents lists available at ScienceDirect

Fuel

journal homepage: www.elsevier.com/locate/fuel

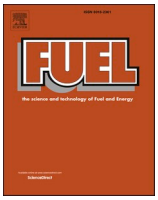

Synergistic effect in co-processing a residue from a transesterification process with vacuum gas oil in fluid catalytic cracking

Abubakar M. Haruna [a,b,*], Will Meredith [a], Colin E. Snape [a]

[a] Department of Chemical and Environmental Engineering, Energy Technologies Building, University of Nottingham, Jubilee Campus, Triumph Road, Nottingham NG7 2TU, UK
[b] Department of Chemical Engineering, Ahmadu Bello University (A.B.U), Zaria, Nigeria

ARTICLE INFO

Keywords:
FCC
Co-processing
Bio-oil
Waste oils
Vacuum gas oil

ABSTRACT

The catalytic co-processing of bottom fuel oil (BFO) with refinery vacuum gas oil (VGO) using a commercial fluid catalytic cracking (FCC) zeolite equilibrium catalyst was carried out to ascertain its potential as a source for biofuels. The BFO used was the distillation residue from biodiesel transesterification process using waste fats and oil; being a mixture of saturated and unsaturated fatty acid methyl esters. The catalytic cracking experiments were performed in a laboratory fixed bed micro activity test (MAT) reactor at 516 °C and atmospheric pressure. As well as the VGO and BFO, three different blends were used with BFO to VGO mass ratios of 10:90, 20:80 and 50:50, and catalyst-to-oil (C/O) ratios of 3.0 – 5.7. The synergistic effect of BFO in VGO blends includes the yield of gasoline, and LPG being higher than predicted for the blends of 10 wt% BFO in VGO. Also, the formation of more CO_2 with the increase in BFO blend level suggests CO_2 production through decarboxylation reactions as a possible route. The compositions of the produced gasoline for pure VGO and 10 wt% BFO are similar as well. The cracking of 10 wt% BFO gives a higher fraction of aromatics, alkenes and naphthenes than other blends. However, some deterioration was observed when higher substitution levels of BFO were used, resulting in a decrease in the gasoline yield and higher yields of LCO, HCO and coke as predicted. Overall, co-processing BFO with VGO may be economically attractive because the BFO is obtained from waste oils and fats which are one of the under-exploited sources of biodiesel feedstocks and add value to waste management.

1. Introduction

Renewable and sustainable energy sources are much in demand because of the deteriorating effect of burning fossil fuels; emitting greenhouse gases (GHGs) and causing global warming [1]. Disastrous consequences related to GHGs emissions have caused the U.S about $1.975 trillion [2], and the UK, between £1.3 and £1.9 billion [3]. One favourable source of alternative energy is liquid biofuel (obtained from bio-oil), which can address the environmental issues of GHGs emissions, particularly CO_2, connected with fossil fuels. However, for biofuels to be accepted as a substitute for fossil fuels they must meet certain stringent regulations employed by policymakers. European Union (EU) underpins sustainability criteria including the negative direct impact that the production of biofuels may have due to indirect land-use change (ILUC) [4]. Targets were also set by the EU for a 10% cut of renewables in the transport sector and 20% energy from renewables by 2020 [5].

One major challenge of bio-oil is that, unlike fossil oil which is predominately hydrocarbon in nature, it is a complex mixture of hydrocarbons, anhydrous sugars, aldehydes, ketones, and phenols, organic acids and high oxygen content [6]. The high concentration of oxygenates in bio-oil [7] makes their direct use as biofuels difficult; the high water content lowers their heating value; they polymerize when heated, and have high acidity leading to their instability during storage and high polarity making them immiscible with fossil oil. Therefore, upgrading bio-oil is a necessity for it to be utilized in processes that produce drop-in fuel.

Catalytic pyrolysis [8–10] and hydrotreating have been proven to reduce the oxygen contents of bio-oils. The former uses a zeolite catalyst that enables both pyrolysis and bio-oil upgrading to take place in a single run [11], and the latter uses hydrogen in the presence of a metal catalyst where almost all the oxygen in the bio-oil can be removed when sufficient hydrogen amounts are used [12]. However, the use of costly hydrogen from petroleum oil alongside additional capital expenditure makes the process unattractive.

* Corresponding author.
E-mail address: abuharuun@yahoo.com (A.M. Haruna).

https://doi.org/10.1016/j.fuel.2022.124973
Received 1 April 2022; Received in revised form 7 June 2022; Accepted 19 June 2022

A better and more sustainable way would be to utilise the existing oil refinery infrastructure and use it to produce biofuels from renewable resources [13–16] and so potentially avoid high capital costs for constructing new plants. For example, bio-oils could be blended with vacuum gas oil (VGO) in fluid catalytic cracking (FCC) units. Here there is the potential to lower oxygen contents through decarboxylation, decarbonylation and dehydration reactions in the form of CO_2, CO and H_2O [17]. However, this comes with negative consequences including poor yields of hydrocarbons and a high coke yield. The heat of the endothermic reaction is provided by burning the coke on the catalyst, which may affect the heat balance of FCC reactions. Fig. 1 shows the biomass and waste oils valorization routes including; catalytic fast pyrolysis, fast pyrolysis, hydrotreating, and transesterification and their link with the FCC unit. A potential feed is bottom fuel oil (BFO) residue; a heavier component produced during the continuous distillation process of biodiesel production from waste vegetable fats and oils and this could be co-processed with VGO in the FCC unit to produce biofuels.

One of the main reactions in the FCC reactor is the cleaving aliphatic C–C of bonds to help produce high-octane gasoline. Aromatics are more stable, cracking only their aliphatic side chains which also leads to coke formation that deactivates catalysts [18]. Other reactions that contribute to the product's yield and quality include hydrogen transfer, dehydrogenation of cycloalkanes and isomerization of intermediate carbenium ions [19]. Huber [14] suggested that the transformation of oxygenate compounds from bio-oil in the FCC reactor occurs mainly via a sequence of five classes of reactions including; cracking of oxygenates, dehydration, condensation reactions, hydrogen-producing and hydrogen consuming reactions. Also, there may be hydrogen formation through decarbonylation, and dehydrogenation of the bio-oil. Hydrogen may be consumed by transfer to a dehydrated molecule through hydrogen transfer, hydrogenation and decarbonylation reactions [20] between two hydrocarbons which take place on acid sites. Decarboxylation and decarbonylation reactions also occur in the co-processing reaction. Through decarbonylation, aldehydes and ketones produce CO to form an upgraded product with a higher hydrogen/carbon (H/C) ratio. Acids react through decarboxylation to form CO_2 and a product with an improved H/C ratio. These reactions can both consume and produce hydrogen by internal hydrogen transfer [21]. Hydrogen transfer, decarbonylation and hydrogenation are the main H/C enriching reactions of the products. Hydrogen transfer involves a hydrogen donor (naphthene) and a hydrogen acceptor (alkene) and when processing bio-oil with predominantly low naphthene an alternative source of hydrogen is required that can improve the H/C ratio of the products [22]. However, some additional reactions have to be considered when CO_2 and CO are produced. Methanation involves the removal of CO_2 and CO through their separate reactions with hydrogen to produce methane and water, and water–gas-shift involves a reaction between CO and water vapour to produce CO_2 and hydrogen [14,21,22]. Also, steam reforming of dehydrated products occurs in cracking reactions to form CO and hydrogen. Consequently, it is difficult to conclude with certainty whether the oxygen removal route is either decarboxylation or decarbonylation.

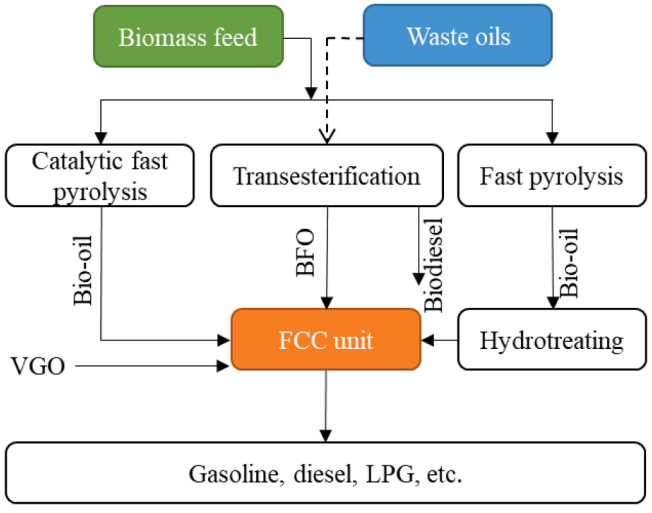

Fig. 1. Biomass and waste oils valorisation routes for co-processing in FCC.

Several reviews, from different perspectives, address the use of oxygenated species in petroleum refineries[13,16,23–31]. While some research was conducted on model compounds of bio-oil [22,32–36], others explored routes with different bio-oils containing 13 to 61% oxygen for co-processing in FCC including waste cooking oil [37–41], fast pyrolysis oil [42–48], catalytic pyrolysis oil [12 49,50], hydrodeoxygenated oil [15,51–54], and hydrothermal liquefaction oil [55]. But, none of the routes could be concluded to be the best choice as it depends on the objective of the co-processing route. Though the results showed that up to 10 – 20% bio-oil could be blended in the FCC unit without much deterioration in the products.

In this study, the potential of using a BFO residue from a transesterification process, without any pre-treatment, to produce biofuels and their synergistic effect in co-processing with VGO is evaluated using a micro activity test (MAT) set-up and a commercial FCC equilibrium catalyst. The level to which BFO could be incorporated into the FCC reactor by co-processing with VGO was investigated using three bio-oil blends and cracking severity was carried out at three different catalysts to oil ratios. The co-processing results in terms of product yield distribution and conversion are equated with those from the cracking of individual feeds (BFO, VGO).

2. Experimental

2.1. Feed properties

The VGO was collected based on the standard for sampling industrial chemicals (ASTM E300) [56] from a commercial refinery. The BFO used was supplied by the Argent energy. The BFO was stored in a freezer to maintain its stability and was later used in the reactor as received without any pre-treatment. Three blends of 10, 20 and 50 wt% BFO in VGO were used.

The feedstocks were characterized by simulated distillation (SIMDIS) according to ASTM D2887 and by elemental analysis, using Carlo Elba Leco CHNS628, to determine the contents of C, H, N, and S, where the O content is obtained by difference. The distributions of the chemical components in both the VGO and BFO were obtained using GC–MS Agilent (7890B GC; 5977A MSD). To easily identify the compounds with lower concentrations that might not be resolved, the feedstocks were separated into aliphatics, aromatics and polar fractions by the modified open column chromatographic method (ASTM 2549). The high heating values (HHV) were determined using the IKA C5000 bomb calorimeter (IKA LABORTECHNIK), while viscosity measurement was carried out using Brookfield DV-II + Pro viscometer at 50 °C and 100 °C. Properties of the feedstocks are given in Table 1 and their detailed compositional analysis is in the Supplementary Information Table S1.

2.2. Catalyst properties

A commercial FCC zeolite equilibrium catalyst (E-cat) was used. The catalyst originally supplied by BASF has a Lewis and Bronsted acidity of 2.51 and 0.2 (μmol/m^2) respectively. The catalyst was dried in an oven at 105 °C for 4 h and thermally calcined in a tube furnace to burn off the carbonaceous deposits. The surface area, pore volume and average pore size of the calcined catalysts were analysed based on isothermal adsorption of nitrogen using the Micro metrics TriStar instrument with samples degassed at 200 °C for 3 h. The standard Brunauer-Emmett-Teller (BET) and Barret-Joyner-Halenda (BJH) methods were used to calculate the surface area and pore size distribution of the catalysts [57].

Table 1
Properties of the VGO and BFO.

		VGO	BFO
Kinematic viscosity (cst)	at 50 °C	25.4	
	at 100 °C	6.73	
Elemental analysis (wt.%)			
Carbon		85.6	76.3
Hydrogen		12.4	11.9
Nitrogen		1.3	2.4
Sulfur		0.3	0.2
Oxygen (by difference)		0.5	9.2
Composition (wt.%), ASTM 2549			
Aliphatics		71.9	
Aromatics		15.8	
Polar		12.3	
HHV (MJ/kg)		43.0	40.3
H/C		1.7	1.6
GCMS method (area %)			
Octadecenoic acid methyl ester		21.0	
Octadecanoic acid methyl ester		17.2	
Eicosenoic acid methyl ester		6.9	
Tetracosanoic acid methyl ester		9.9	
9-Octadecenamide		13.8	
Octadecanamide		7.4	
Myristamide		6.2	
Cholesterol		4.6	
Simulated distillation (°C), D2887			
Initial boiling point		204	331
10%		302	369
25%		365	423
50%		426	522
70%		462	570
90%		519	600
Final boiling point		600	700

The matrix surface area was calculated using the t-plot method, while the zeolite surface area was calculated by taking the difference between the BET surface area and the matrix surface area. Table 2 shows the textural properties of the catalyst.

2.3. FCC reactor and procedure

The cracking reactions were conducted in a fixed-bed micro activity test (MAT) reactor that was placed in an electric furnace as shown in Fig. 2, according to the ASTM D-3907/D5154 method [58,59]. The reactor was made of quartz and has a height of 35 cm and a diameter of 1.6 cm. During each experiment, 4 g of the catalyst was placed inside the reactor supported by a glass wool bed and the reaction took place under atmospheric pressure. Before starting the experiment, nitrogen gas was used to purge the reactor at a rate of 40 ml.min^{-1} for 20 min to remove residual oxygen. After that, a certain quantity of standard gas oil feedstock was injected using a plunger syringe pump into the hotbed of the catalyst. Each reaction cycle takes 75 s of cracking at 516 ℃ and 15 min of stripping under nitrogen flow. This condition is controlled using proportional integral derivative (PID) temperature control with thermocouples placed inside the furnace positioned within the internal wall and another thermocouple positioned just above the catalyst bed to measure inside reactor temperature. The thermal vapours then contact the catalyst where cracking is induced on the vapour by the catalyst bed which is supported by glass wool. During the experiment, nitrogen gas was used to remove the reaction vapour into the condensing system cooled at 5 °C where condensable volatiles are collected as the liquid product in a glass receiver, then stored in a sealed vial and refrigerated for later analysis. The non-condensable gases are collected with the aid of a 1 Litre gas-tight bag for immediate analysis, while the deactivated or coked catalyst is collected from the reactor after cooling down.

Table 2
Properties of the FCC equilibrium catalyst.

Catalyst properties	Equilibrium catalyst
BET total surface area (m^2/g)	131
t-plot (matrix surface) micropore area (m^2/g)	93
Zeolite surface area (m^2/g)	38
t-plot micropore volume (cm^3/g)	0.036
BJH mesopore volume (cm^3/g)	0.109
Average pore diamter (nm)	4.97

Five sets of experiments were carried out over the FCC equilibrium catalyst using the two feedstocks and by three catalyst-to-oil (cat/oil) ratios, so thirteen experiments were carried out, each one in triplicate.

(i) 100 wt% VGO catalytic cracking using cat/oil ratios of 3.1, 4.7 and 5.6
(ii) 10 wt% BFO in VGO co-processing using cat/oil ratios of 3.0, 4.1 and 5.1
(iii) 20 wt% BFO in VGO co-processing using cat/oil ratios of 3.0, 4.1 and 5.4
(iv) 50 wt% BFO in VGO co-processing using cat/oil ratios of 2.6
(v) 100 wt% BFO catalytic cracking using cat/oil ratios of 3.0, 4.2 and 5.7

The C/O ratios were obtained by keeping the amount of catalyst constant and changing the amount of oil pumped into the reactor; to vary the level of conversion. The quality of the test was determined by calculating the mass recoveries which fell in the range of 90–101 %. Individual hydrocarbons were grouped based on the standard FCC procedure and using simulated distillation (SIMDIS) test method D2887: dry gases ($C_1 - C_2$), liquefied petroleum gas (LPG: $C_3 - C_4$), gasoline ($C_5 - C_{12}$), light cycle oil (LCO: $C_{13} - C_{20}$), heavy cycle oil (HCO: C_{20+}) and coke. In refining industries, conversion is defined as a sum of the yields of more desirable products including; dry gas, LPG, gasoline and coke.

$$Yield\ \ of\ \ ith\ \ product = \frac{\text{mass of } i\text{th product}}{\text{mass of oil feed}}$$

$$Conversion = Yield\ \ of\ (dry\ \ gases + LPG + gasoline + coke)$$

$$Mass\ \ balance(recovery) = \frac{\sum \text{all products}}{\text{mass of oil feed}} X100\% = \frac{\text{output}}{\text{input}} X100\%$$

Liquid products were analysed utilizing an Agilent GC–MS (7890B GC; 5977A MSD), with a single quadrupole mass spectrometer and an electron impact ionization detector (EI). The GC injector was kept at 280 °C, and the injection split ratio and the injection volume were 10:1 and 1 μL, respectively. The condensable products were separated with a DB-1701 MS column (60 m × 0.25 mm i.d. × 0.5 μm film thickness). The liquid compositions were identified by comparing all chromatogram spectra to the national institute for standards and testing (NIST) mass spectral search program and the Wiley mass spectrum library.

Gases generated during the experiments were immediately analysed on a Clarus 580 gas chromatograph (GC) fitted with a flame ionization detector (FID) and thermal conductivity detector (TCD) operating at 200 °C. Five millilitres (mL) of gas sample was introduced to the GC for hydrocarbon and non-hydrocarbon analysis. The hydrocarbon gases were analysed by injecting 100 μL of gas samples (split ratio 10:1) onto the FID with separation performed on an alumina plot fused silica (30 m × 0.32 mm × 10 μm) column, with helium as the carrier gas. The oven temperature was programmed from 60 °C (13 min hold) to 180 °C (10 min hold) at 10 °C min^{-1}. The non-hydrocarbon gases (H_2, H_2S CO and CO_2) were analysed by injecting 500 μL onto the TCD. Separation was performed on a Haysep N6 packed column (60–80, 7 × 1/8_sulfinert), using Argon as the carrier gas.

3. Results and discussion

3.1. Repeatability

The yields of coke, liquid and gases obtained from all the

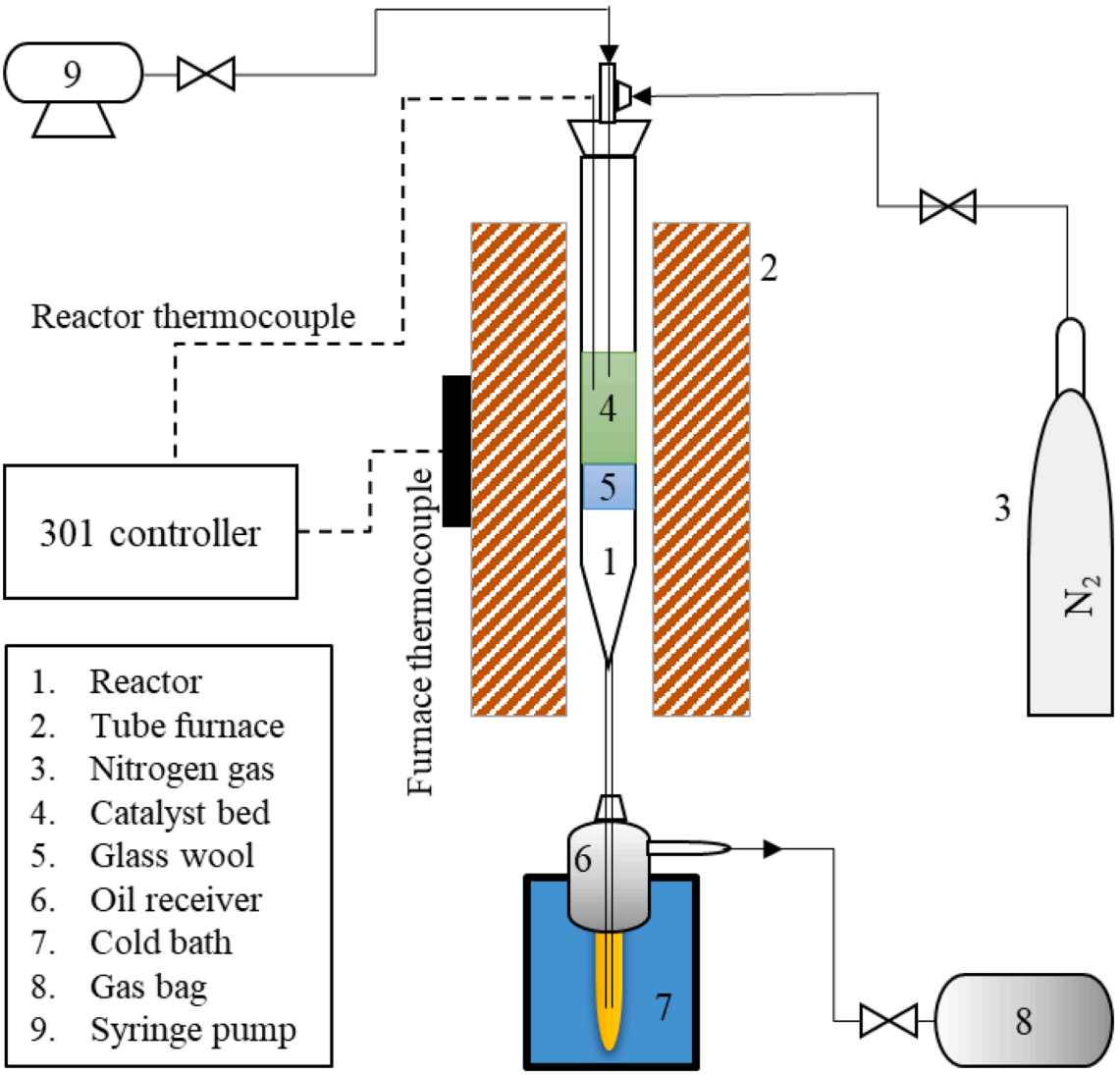

Fig. 2. Catalytic cracking micro activity test set-up.

experiments are presented in Figure S1 in the Supplementary Information. For triplicate tests for each experiment, the test with the highest recovery of products is presented, but the recovery of all products from the initial feed is at least 90 wt% in all cases. Similarly, the mean values of product yields are shown in Figure S2 in the Supplementary Information. Each bar represents a single product while the error bars represent the standard deviation of each combined yield calculated over three trials. The standard deviations for the liquid and coke yields were within the ranges of 0.3 – 5.5 % and 0.1 – 1.3 % on a feed basis, respectively. However, there is a larger standard deviation for the gas yields which are within the range of 2.8 – 15.3 % which was due to losses during the storage period.

3.2. *Distribution of catalytic cracking product yields*

As shown in Fig. 3, the overall conversions of pure VGO, BFO and their blends increase with an increase in catalyst to oil (C/O) ratios. Pure BFO was used in its raw form without any pre-treatment, hence, its conversion is distinctly lower than pure VGO, and their blends. While the addition of BFO reduces the conversion at all C/O ratios, a maximum conversion of 63.6 % and 60.4 % was achieved for the 10 and 20 wt% BFO blends at a C/O of 4.1 respectively, which represents an increase of 2.6 % and a decrease of 1 % from the conversion obtained using pure VGO. Furthermore, a minimum conversion of 39.3 % was achieved for

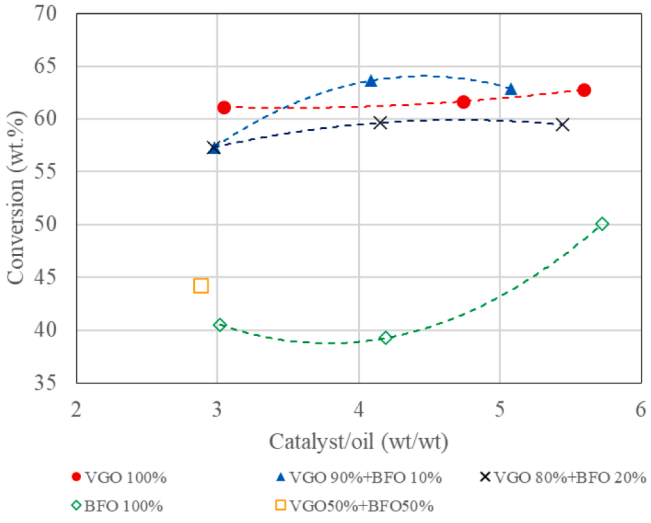

Fig. 3. Conversion as a function of the catalyst to oil ratio for the different feed blend ratios.

the pure BFO at a C/O ratio of 4.1, representing a decrease of 22 % from the value obtained using pure VGO.

A comparison of coke forming potential of pure VGO, BFO and the blends of 10, 20, and 50 wt% BFO in VGO is displayed in Fig. 4. Fig. 4 (a) shows an increase in coke yield with an increase in C/O ratios; even though there is a relatively little difference in coke production in cracking pure BFO, 10, 20 and 50 wt% BFO in VGO as the C/O ratio increases, except for the pure VGO that has the lowest coke yield as expected. To have a clearer view of this effect, coke yields from different feeds were compared with conversion (Fig. 4b). The coke yields increase sharply with conversion and with the level of BFO blends in VGO, where the VGO recorded minimum coke yield. For the lowest conversion just above 45 wt%, BFO resulted in the highest yield of coke, while the 10 wt % BFO blend gave a similar coke yield to the VGO. The coke yields in this paper range from 3 to 6 wt%, which is comparable to the yield of 3 – 8 wt % obtained from MAT reactor published literature [50,52–54,60].

The co-processing ability of bio feedstocks in FCC is better understood by looking at the synergistic effects [61,62]. The synergy between the VGO and BFO can be examined by comparing product yields with conversion for the cracking of VGO, BFO and their different blends as displayed in Fig. 5. In Fig. 5 (a), the gasoline yield of all the feeds tested decreases with an increase in conversion, where the maximum gasoline yield of BFO is reached at a lower conversion of 41 wt% than the cracking of VGO (62 wt%) and the 10 and 20 wt% BFO (58%). Increasing the severity of the cracking reaction above these conversion levels suppresses liquid product yield and enhances the formation of more gaseous products. VGO cracking gives the highest gasoline yield which slightly reduces as the blend ratio of the co-processing with BFO increases from 10%, 20% and 50%.

The yield of light cycle oil (LCO), which represents the diesel fraction of the feed, decreases with conversion as well as with increasing BFO blend ratios shown in Fig. 5 (c). As explained earlier, the BFO feed is a distillation residue of biodiesel production, hence its cracking gives the highest yield of LCO with a maximum achieved at a conversion of about 42 wt% and for higher conversions obtained in the BFO blends and VGO. At higher conversion levels, the cracking of LCO to gasoline and gases is enhanced. A similar trend is observed in heavy cycle oil (HCO) yield (Fig. 5d) for the cracking of individual BFO and VGO, however, HCO yields for the BFO blends (10 and 20 wt%) were lower than predicted, again reflecting synergy in BFO cracking. The fact that the yields of desirable gasoline and LCO are higher compared to the HCO is an encouraging result that is similar to the one obtained from the literature [90, 97].

Fig. 5 (b) shows the liquified petroleum gas (LPG) yield for the catalytic cracking of the BFO, VGO and their blends increases markedly with conversion. The LPG yield is lower from the BFO than the VGO due to the selectivity of deoxygenation reactions of BFO forming CO, CO_2 and dry gas. However, the LPG yield for the cracking of the 10 and 20 wt % BFO blends is higher than predicted. It is worthy to note that bio-oil compositional variations may alter the relative yield of LPG and dry gas in co-processing reaction and results from comparison will be challenging [36,49].

The dry gas yield in Fig. 5 (e) is higher from the BFO than the VGO and increases with the conversion possibly due to methane being formed from cracking the methyl esters. However, the dry gas yields for the coprocessing of 10 and 20 wt% BFO are lower than predicted, with the yield of 10 wt% BFO close to that for the VGO. The yields of CO_2 and CO are shown in Fig. 5 (f) and (g). The yield of CO_2 from the BFO mixtures increases slightly with the blend ratio compared to pure VGO, especially the 10 wt% BFO seems to converge with that of VGO at a conversion above 62 wt%. However, when the BFO blend ratio is increased to 50 wt % the CO_2 yield increases closer to that of pure BFO. Interestingly, VGO has a relatively highest yield of CO than other feeds which increases with conversion. However, the yields of BFO blend are lower than the individual craking of VGO and BFO. This result further suggests that deoxygenation of BFO follows the decarboxylation route where oxygen is removed in form of CO_2 rather than CO, which is attractive because two atoms of oxygen are removed compared to one atom of oxygen as CO.

The hydrogen gas yield (Fig. 5h) increases with conversion and BFO gives a higher yield than VGO. However, the hydrogen yield of the BFO mixtures is higher than that of either pure BFO or VGO cracking, indicating that either hydrogen is not consumed in a synergistic reaction or hydrogen formation was favoured.

An overview of product yields for the cracking of VGO, BFO and the blends is shown in Fig. 6. The yield of gasoline is highest followed by LCO, LPG, HCO, coke, dry gas, CO_2 and CO. Similarly, the yield for the blends of 10 and 20 wt% BFO for LPG is higher than what would be expected from the additive mixture of the individual feeds (VGO and BFO), symbolizing the effect of co-processing synergy. Furthermore, there is a higher gasoline yield than expected from the additive mixture for the blend of BFO 10 wt% due to the synergistic effect. Therefore, co-processing of BFO above 10 wt% reduces gasoline yield due to the presence of more oxygenated compounds that are selective to deoxygenation reactions. The cracking of 10 wt% BFO shows that LCO and coke yields were purely additive and increased with the BFO blend levels. Conversely, the yield for all the blends in the cracking of HCO was lower than expected showing an antagonistic effect in co-processing BFO blends with VGO. The yield of CO_2 for the cracking of the BFO blends is higher compared to that of CO, indicating the impact of dehydration, decarboxylation, and decarbonylation reactions of the oxygenated compounds when mixed with VGO.

3.3. Liquid phase chemical composition

The overall liquid phase product distribution involving gasoline, LCO, and HCO was based on a quantitative method of simulated distillation. For detailed qualitative information on the chemical composition of the liquid phase, GC–MS analysis was performed. The compounds are classified into the following groups: aliphatics, mono-, di-, and tri-aromatics (Fig. 7). Detailed liquid product compositional analysis can

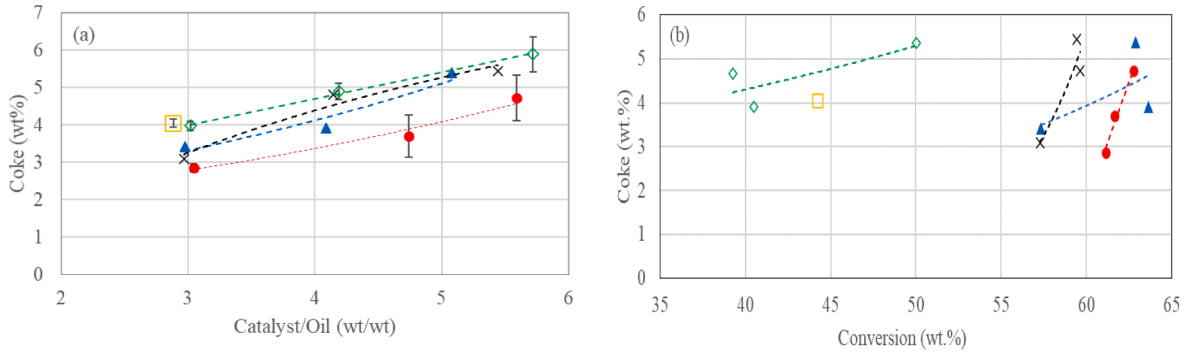

Fig. 4. Dependency of coke yield on (a) catalyst to oil ratio and (b) conversion for 100% VGO (●), 10% BFO (▲), 20% BFO (x), 50% BFO (□) and 100% BFO (◊).

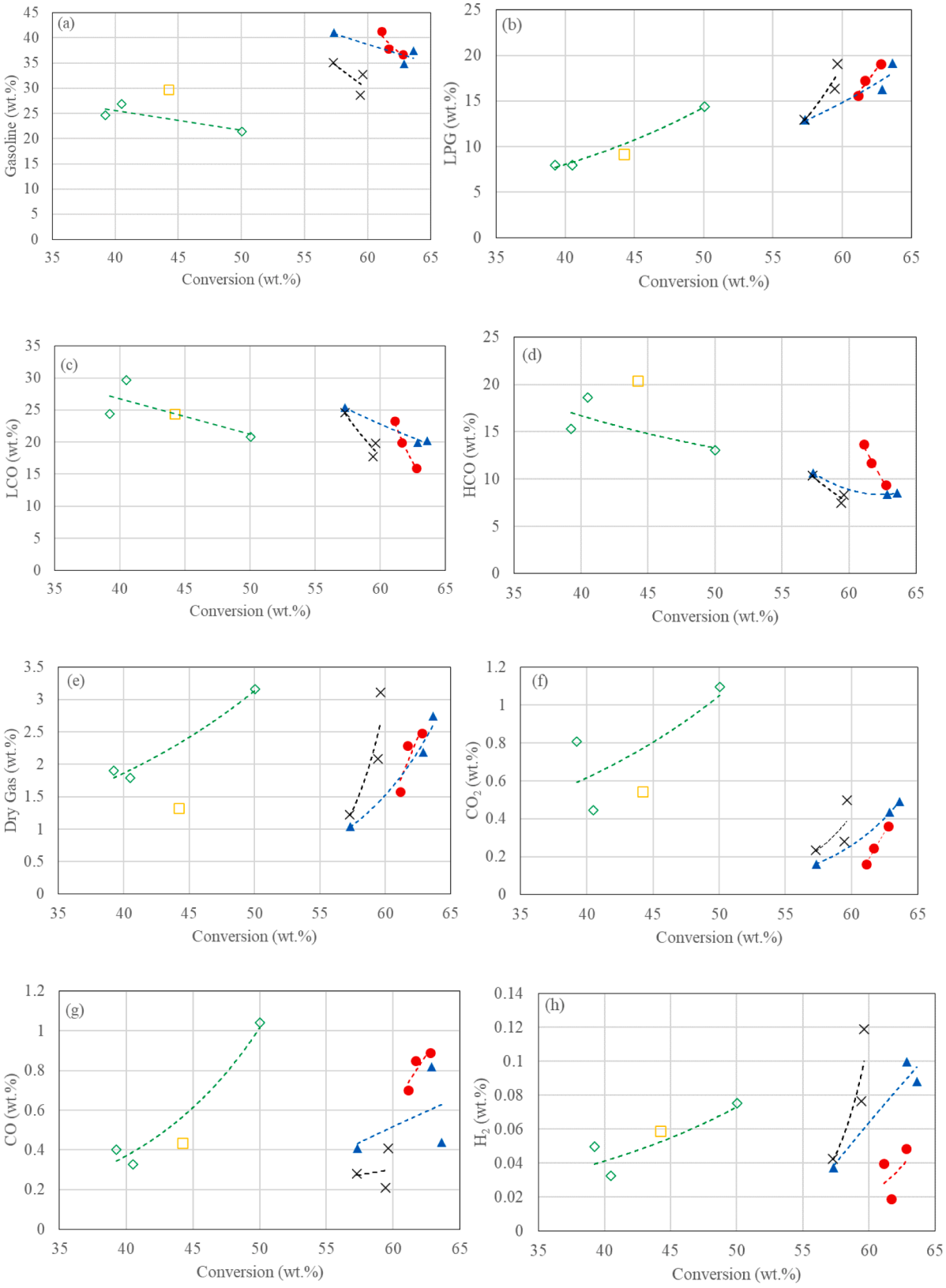

Fig. 5. Product distribution at different conversions for: 100% VGO (●), 10% BFO (▲), 20% BFO (x), 50% BFO (□) and 100% BFO (◊).

be found in Table S2 of the supplementary information. Likewise, the GC–MS chromatograms for the cracking of VGO, BFO and their blends are displayed in Figures S3 and S4. Figure S3 in the Supplementary Information shows VGO normal distribution of hydrocarbons ranging from hexadecane, and pentacosane to tetratriacontane (C_{16} to C_{34}) and the position of peaks matched to the relative retention time of each constituent molecule based on their different molecular weight and structure. The relative abundance of the aliphatic fractions is more in the

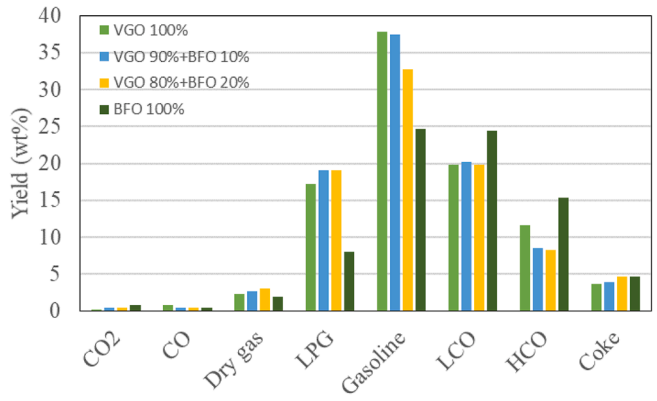

Fig. 6. Overview of product yields in cracking of different feeds at 516 ℃ with a catalyst to oil ratio of 4.1.

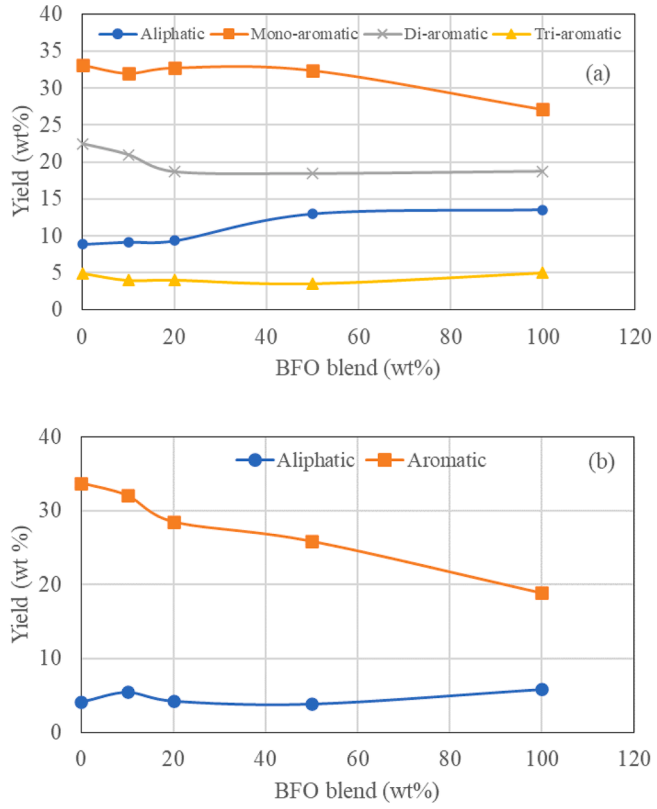

Fig. 7. Aromatic and aliphatic hydrocarbon yields obtain at different BFO blend ratios in the (a) total liquid products and (b) gasoline fractions.

centre of the chromatogram which is predominantly C_{23} – C_{28}.

From Fig. 7 (a), the aromatic yield of the total liquid product decreases with an increase in the BFO blending ratio, while that of aliphatic increases (note that the zero BFO blend represents VGO 100 wt %.) The mono-aromatic, which comprises mainly 1,4-dimethyl benzene or p-xylene, 1-ethyl-3-methyl benzene, and 1,2,4-trimethyl benzene, has the highest yield compared to aliphatic, di-, and tri- aromatics, with a maximum yield for the cracking of BFO 20 wt% blend. The cracking for VGO has a higher yield of mono-, di-aromatic than BFO comprising 1,7-dimethyl naphthalene, 1,6,7-trimethyl naphthalene, and 2-methyl naphthalene. A similar trend is observed for the liquid product distribution within the gasoline range as shown in Fig. 7 (b), with the exception that it does not contain di-(excluding naphthalene) and tri-aromatic compounds. Aromatic yield decreases with an increase in blending ratio, while that of aliphatic increases. Pure VGO achieved the maximum aromatic yield, while pure BFO reached the highest aliphatic yield. Similarly, 10% BFO has the highest aromatic and aliphatic yield including 4-methyl octane, 3-ethyl hexane, and 2-methyl decane.

At about 61% conversion, gasoline yields are comparable for VGO, 10% BFO, and 20% BFO and it is good to check whether the compositions of the gasoline are similar as well. Table 3 breaks down the yields of the major composition classes of the gasoline fractions for the VGO, BFO and their blends into oxygenates, n-alkanes, alkenes, i-alkanes, naphthenes and aromatics. Generally, n-alkanes and *iso*-alkanes increase with the blending ratio, while alkenes, naphthenes and aromatics decrease. The yield of aromatics is higher than all other gasoline components, followed by alkenes, i-alkanes, naphthenes, and alkanes. The cracking of 10 wt% BFO gives a higher fraction of aromatics, alkenes and naphthenes than other blends. Aromatics, alkenes and *iso*-alkanes are identified as the major products of the gasoline fraction. The main alkenes and *iso*-alkanes constituents consist of 3-octene, 2-decene and 4-methyl octane, while the naphthenes include methyl-, dimethyl-, and trimethyl- cyclohexane. One way to explain the high yield of the aromatics in the gasoline fraction is by understanding the composition of both raw VGO and BFO. During catalytic cracking, the dehydrated long-chain olefinic compounds undergo hydride abstraction by carbonium ion leading to a higher degree of unsaturation and formation of trienes. Once trienes are formed, they will rapidly undergo cyclization forming aromatic compounds [19]. Consequently, the formed aromatics continue to react together to form heavier hydrocarbons containing two or more benzene rings.

Also, there is a small amount of oxygenates in the gasoline fraction for cracking of 50 wt% BFO, and pure BFO; including carbonic acid, ethyl-, methyl ester and benzyl isopentyl ether. Interestingly, no unconverted oxygenate compounds were detectable in the gasoline fractions from the 10 and 20 wt% BFO blends due to the low oxygen content (9.2 wt%) of raw BFO. As expected, most of the oxygenates cracked to contribute to higher yields of CO_2.

Table 3
Yields of gasoline range compound from the co-processing of VGO and BFO at a conversion of up to 61 wt% and a catalyst to oil ratio of 4.1 (wt/wt) levels.

	VGO 100%	BFO 10%	BFO 20%	BFO 50 %	BFO 100%
oxygenates				0.38	**1.68**
carbonic acid, ethyl-, methyl ester				0.38	0.27
benzyl isopentyl ether					1.41
n-alkanes	**0.49**	**0.71**	**0.81**	**0.86**	**1.11**
C10	0.09	0.26	0.08	0.50	0.87
C11	0.09	0.08	0.47	0.08	0.08
C12	0.31	0.38	0.26	0.29	0.16
alkenes	**4.35**	**4.26**	**3.79**	**3.24**	**2.91**
C7	3.20	3.43	3.00	2.53	1.48
C8	0.21	0.47	0.44	0.27	0.67
C9	0.09	0.12	0.20	0.22	0.53
C10	0.07	0.09	0.08	0.16	0.15
C12	0.77	0.16	0.08	0.06	0.08
i-alkanes	**2.48**	**2.61**	**2.77**	**2.98**	**3.17**
C8	0.44	0.08	0.14	0.67	0.84
C9	1.32	0.81	1.46	1.42	1.21
C10	0.32	1.03	0.75	0.56	0.85
C11	0.40	0.69	0.43	0.33	0.29
naphthenes	**0.80**	**0.67**	**0.57**	0.48	**0.46**
C7	0.26	0.08	0.17	0.13	0.06
C8	0.31	0.21	0.13	0.04	0.27
C9	0.05	0.26	0.20	0.09	0.07
C10	0.18	0.13	0.07	0.21	0.06
aromatics	**29.71**	**29.21**	**24.78**	**21.77**	**15.37**
C7	2.72	1.87	1.35	1.35	0.16
C8	6.64	6.85	5.87	5.56	3.54
C9	8.84	8.44	7.03	6.74	4.21
C10	10.03	9.94	8.16	6.84	6.04
C11	1.48	2.12	2.38	1.28	1.42

4. Conclusions

The results demonstrated that it is possible to add value to untreated biodiesel distillation residue by converting it to more important gasoline, LPG and LCO in a MAT reactor. The synergistic effect of BFO in VGO blends include the yield of gasoline, LPG being higher than predicted for the blends of 10 wt% BFO in VGO. Also, the formation of more CO_2 with the increase in BFO blend level suggest CO_2 production through decarboxylation reactions as a possible route. The compositions of the produced gasoline for pure VGO and 10 wt% BFO are similar as well. The cracking of 10 wt% BFO gives a higher fraction of aromatics, alkenes and naphthenes than other blends. Furthermore, BFO has been demonstrated to be effective in FCC as no detectable unconverted oxygenate in the gasoline range for the 10 and 20 wt% BFO and has the potential to give less coke formation when blended with VGO. Therefore, cracking of 10 wt% BFO in VGO has the closest yield characteristics compared to pure VGOindicating that it is a favourable blend level that can be co-process under FCC conditions.

Declaration of Competing Interest

The authors declare that they have no known competing financial interests or personal relationships that could have appeared to influence the work reported in this paper.

Acknowledgement

This work was financially supported by IsDB Bank and PTDF. Special thanks must go to the Argent Energy, UK for providing the BFO sample used in this work as well as Nigeria National Petroleum Corporation for the VGO and commercial FCC equilibrium catalyst supply.

Appendix A. Supplementary data

Supplementary data to this article can be found online at https://doi.org/10.1016/j.fuel.2022.124973.

References

[1] A.Schmidt G. 2020 Tied for Warmest Year on Record, NASA Analysis Shows. Natl Aeronaut Sp Adm Release 2021. https://www.giss.nasa.gov/research/news/20210114/ (accessed February 1, 2021).
[2] NOAA. Billion-Dollar Weather and Climate Disasters. NOAA Natl Centers Environ Inf US 2021. 10.25921/stkw-7w73.
[3] Emma Howard Boyd. Climate change impacts and adaptation. UK Environment Agency 2018.
[4] EU. Sustainability criteria. Eur Comm 2020. https://ec.europa.eu/energy/topics/renewable-energy/biofuels/sustainability-criteria_en?redir=1.
[5] EU. 2020 climate & energy package. Eur Comm 2009. https://ec.europa.eu/clima/policies/strategies/2020_en.
[6] A. Pattiya. Chapter 1: Fast pyrolysis. In: Rosendahl L, editor. Direct Thermochem. Liq. Energy Appl., Woodhead publishing; 2018, p. 3–23.
[7] Ibarra Á, Hita I, Arandes JM, Bilbao J. Influence of the Composition of Raw Bio-Oils on Their Valorization in Fluid Catalytic Cracking Conditions. Energy Fuels 2019;33:7458–65. https://doi.org/10.1021/acs.energyfuels.9b01527.
[8] Agblevor FA, Beis S, Mante O, Abdoulmoumine N. Fractional catalytic pyrolysis of hybrid poplar wood. Ind Eng Chem Res 2010;49:3533–8. https://doi.org/10.1021/ie901629r.
[9] Gayubo AG, Valle B, Aguayo AT, Olazar M, Bilbao J. Olefin production by catalytic transformation of crude bio-oil in a two-step process. Ind Eng Chem Res 2010;49:123–31. https://doi.org/10.1021/ie901204n.
[10] Staser J. DOE Bioenergy Technologies Office (BETO) 2019 Project Peer Review. Beto 2019:1–19.
[11] Pattiya A. Chapter 2: Catalytic pyrolysis. In: Rosendahl L, editor. Direct Thermochem. Liq. Energy Appl., Woodhead publishing; 2018, p. 29–55.
[12] Lindfors C, Paasikallio V, Kuoppala E, Reinikainen M, Oasmaa A, Solantausta Y. Co-processing of dry bio-oil, catalytic pyrolysis oil, and hydrotreated bio-oil in a micro activity test unit. Energy Fuels 2015;29:3707–14. https://doi.org/10.1021/acs.energyfuels.5b00339.
[13] Bertero M, Sedran U. Coprocessing of Bio-oil in Fluid Catalytic Cracking. Elsevier BV 2015. https://doi.org/10.1016/B978-0-444-63289-0.00013-2.
[14] Huber GW, Corma A. Synergies between bio- and oil refineries for the production of fuels from biomass. Angew Chemie - Int Ed 2007;46:7184–201. https://doi.org/10.1002/anie.200604504.
[15] de Miguel MF, Groeneveld MJ, Kersten SRA, Way NWJ, Schaverien CJ, Hogendoorn JA. Production of advanced biofuels: Co-processing of upgraded pyrolysis oil in standard refinery units. Appl Catal B Environ 2010;96:57–66. https://doi.org/10.1016/j.apcatb.2010.01.033.
[16] Bezergianni S, Dimitriadis A, Kikhtyanin O, Kubička D. Refinery co-processing of renewable feeds. Prog Energy Combust Sci 2018;68:29–64. https://doi.org/10.1016/j.pecs.2018.04.002.
[17] D. Castello LR. Chapter 9: Coprocessing of pyrolysis oil in refineries. Direct Thermochem. Liq. Energy Appl., Lasse Rosendahl; 2018, p. 293–317.
[18] Cerqueira HS, Caeiro G, Costa L, Ramôa RF. Deactivation of FCC catalysts. J Mol Catal A Chem 2008;292:1–13. https://doi.org/10.1016/j.molcata.2008.06.014.
[19] Gates BC, Katzer JR, Schuit G. Chemistry of Catalytic Processes. New York: McGraw-Hill, Inc.; 1979.
[20] Pujro R, Panero M, Bertero M, Sedran U, Falco M. Hydrogen Transfer between Hydrocarbons and Oxygenated Compounds in Coprocessing Bio-Oils in Fluid Catalytic Cracking. Energy Fuels 2019;33:6473–82. https://doi.org/10.1021/acs.energyfuels.9b01133.
[21] Donnis B, Egeberg RG, Blom P, Knudsen KG. Hydroprocessing of bio-oils and oxygenates to hydrocarbons. Understanding the reaction routes Top Catal 2009;52:229–40. https://doi.org/10.1007/s11244-008-9159-z.
[22] Corma A, Huber GW, Sauvanaud L, O'Connor P. Processing biomass-derived oxygenates in the oil refinery: Catalytic cracking (FCC) reaction pathways and role of catalyst. J Catal 2007;247:307–27. https://doi.org/10.1016/j.jcat.2007.01.023.
[23] Valle B, Remiro A, García-Gómez N, Gayubo AG, Bilbao J. Recent research progress on bio-oil conversion into bio-fuels and raw chemicals: a review. J Chem Technol Biotechnol 2019;94:670–89. https://doi.org/10.1002/jctb.5758.
[24] Talmadge MS, Baldwin RM, Biddy MJ, McCormick RL, Beckham GT, Ferguson GA, et al. A perspective on oxygenated species in the refinery integration of pyrolysis oil. Green Chem 2014;16(2):407–53.
[25] Cheng S, Wei L, Zhao X, Julson J. Application, deactivation, and regeneration of heterogeneous catalysts in bio-oil upgrading. Catalysts 2016;6(12):195.
[26] Darda S, Papalas T, Zabaniotou A. Biofuels journey in Europe: Currently the way to low carbon economy sustainability is still a challenge. J Clean Prod 2019;208:575–88. https://doi.org/10.1016/j.jclepro.2018.10.147.
[27] Degnan TF, Chitnis GK, Schipper PH. History of ZSM-5 fluid catalytic cracking additive development at Mobil. Microporous Mesoporous Mater 2000;35–36:245–52. https://doi.org/10.1016/S1387-1811(99)00225-5.
[28] Baloch HA, Nizamuddin S, Siddiqui MTH, Riaz S, Jatoi AS, Dumbre DK, et al. Recent advances in production and upgrading of bio-oil from biomass: A critical overview. J Environ Chem Eng 2018;6(4):5101–18.
[29] Kabir G, Hameed BH. Recent progress on catalytic pyrolysis of lignocellulosic biomass to high-grade bio-oil and bio-chemicals. Renew Sustain Energy Rev 2017;70:945–67. https://doi.org/10.1016/j.rser.2016.12.001.
[30] Yáñez É, Meerman H, Ramírez A, Castillo É, Faaij A. Assessing bio-oil co-processing routes as CO2 mitigation strategies in oil refineries. Biofuels, Bioprod Biorefining 2021;15:305–33. https://doi.org/10.1002/bbb.2163.
[31] van Dyk S, Su J, Mcmillan JD, Saddler J (John). Potential synergies of drop-in biofuel production with further co-processing at oil refineries. Biofuels, Bioprod Biorefining 2019;13:760–75. 10.1002/bbb.1974.
[32] Chen G, Zhang R, Ma W, Liu B, Li X, Yan B, et al. Catalytic cracking of model compounds of bio-oil over HZSM-5 and the catalyst deactivation. Sci Total Environ 2018;631-632:1611–22.
[33] Iliopoulou EF, Stefanidis SD, Kalogiannis KG, Delimitis A, Lappas AA, Triantafyllidis KS. Catalytic upgrading of biomass pyrolysis vapors using transition metal-modified ZSM-5 zeolite. Appl Catal B Environ 2012;127:281–90. https://doi.org/10.1016/j.apcatb.2012.08.030.
[34] Güleç F, Meredith W, Sun CG, Snape CE. A novel approach to CO2 capture in Fluid Catalytic Cracking—Chemical Looping Combustion. Fuel 2019;244:140–50. https://doi.org/10.1016/j.fuel.2019.01.168.
[35] Bertero M, de la Puente G, Sedran U. Products and coke from the conversion of bio-oil acids, esters, aldehydes and ketones over equilibrium FCC catalysts. Renew Energy 2013;60:349–54. https://doi.org/10.1016/j.renene.2013.04.017.
[36] Ibarra Á, Palos R, Arandes JM, Olazar M, Bilbao J, de Lasa H. Synergy in the Cocracking under FCC Conditions of a Phenolic Compound in the Bio-oil and a Model Compound for Vacuum Gasoil. Ind Eng Chem Res 2020;59(17):8145–54.
[37] Le-Phuc N, Tran TV, Phan TT, Ngo PT, Ha QLM, Luong TN, et al. High-efficient production of biofuels using spent fluid catalytic cracking (FCC) catalysts and high acid value waste cooking oils. Renew Energy 2021;168:57–63.
[38] Melero JA, Calleja G, Garcia A, Clavero M, Hernandez EA, Miravalles R, et al. Storage stability and corrosion studies of renewable raw materials and petrol mixtures: A key issue for their co-processing in refinery units. Fuel 2010;89(3):554–62.
[39] Nugroho YK, Zhu L. Platforms planning and process optimization for biofuels supply chain. Renew Energy 2019;140:563–79. https://doi.org/10.1016/j.renene.2019.03.072.
[40] Wang Y, Cao Y, Li J. Preparation of biofuels with waste cooking oil by fluid catalytic cracking: The effect of catalyst performance on the products. Renew Energy 2018;124:34–9. https://doi.org/10.1016/j.renene.2017.08.084.
[41] Atabani AE, Shobana S, Mohammed MN, Uğuz G, Kumar G, Arvindnarayan S, et al. Integrated valorization of waste cooking oil and spent coffee grounds for biodiesel production: Blending with higher alcohols, FT–IR, TGA. DSC and NMR characterizations Fuel 2019;244:419–30.
[42] Pinho ADR, De Almeida MBB, Mendes FL, Ximenes VL, Casavechia LC. Co-processing raw bio-oil and gasoil in an FCC Unit. Fuel Process Technol 2015;131:159–66. https://doi.org/10.1016/j.fuproc.2014.11.008.

[43] Wang C, Venderbosch R, Fang Y. Co-processing of crude and hydrotreated pyrolysis liquids and VGO in a pilot scale FCC riser setup. Fuel Process Technol 2018;181:157–65. https://doi.org/10.1016/j.fuproc.2018.09.023.
[44] Ibarra Á, Veloso A, Bilbao J, Arandes JM, Castaño P. Dual coke deactivation pathways during the catalytic cracking of raw bio-oil and vacuum gasoil in FCC conditions. Appl Catal B Environ 2016;182:336–46. https://doi.org/10.1016/j.apcatb.2015.09.044.
[45] Pinho ADR, De Almeida MBB, Mendes FL, Ximenes VL. Production of lignocellulosic gasoline using fast pyrolysis of biomass and a conventional refining scheme. Pure Appl Chem 2014;86:859–65. https://doi.org/10.1515/pac-2013-0914.
[46] Ibarra Á, Rodríguez E, Sedran U, Arandes JM, Bilbao J. Synergy in the Cracking of a Blend of Bio-oil and Vacuum Gasoil under Fluid Catalytic Cracking Conditions. Ind Eng Chem Res 2016;55:1872–80. https://doi.org/10.1021/acs.iecr.5b04502.
[47] Pinho AdR, de Almeida MBB, Mendes FL, Casavechia LC, Talmadge MS, Kinchin CM, et al. Fast pyrolysis oil from pinewood chips co-processing with vacuum gas oil in an FCC unit for second generation fuel production. Fuel 2017;188:462–73.
[48] Ibarra Á, Hita I, Azkoiti MJ, Arandes JM, Bilbao J. Catalytic cracking of raw bio-oil under FCC unit conditions over different zeolite-based catalysts. J Ind Eng Chem 2019;78:372–82. https://doi.org/10.1016/j.jiec.2019.05.032.
[49] Thegarid N, Fogassy G, Schuurman Y, Mirodatos C, Stefanidis S, Iliopoulou EF, et al. Second-generation biofuels by co-processing catalytic pyrolysis oil in FCC units. Appl Catal B Environ 2014;145:161–6.
[50] Gueudré L, Thegarid N, Burel L, Jouguet B, Meunier F, Schuurman Y, et al. Coke chemistry under vacuum gasoil/bio-oil FCC co-processing conditions. Catal Today 2015;257:200–12.
[51] Le-Phuc N, Ngo PT, Ha QLM, Tran TV, Phan TT, Luu LC, et al. Efficient hydrodeoxygenation of guaiacol and fast-pyrolysis oil from rice straw over PtNiMo/SBA-15 catalyst for co-processing in fluid catalytic cracking process. J Environ Chem Eng 2020;8(2):103552.
[52] Fogassy G, Thegarid N, Toussaint G, van Veen AC, Schuurman Y, Mirodatos C. Biomass derived feedstock co-processing with vacuum gas oil for second-generation fuel production in FCC units. Appl Catal B Environ 2010;96:476–85. https://doi.org/10.1016/j.apcatb.2010.03.008.
[53] Fogassy G, Thegarid N, Schuurman Y, Mirodatos C. The fate of bio-carbon in FCC co-processing products. Green Chem 2012;14:1367–71. https://doi.org/10.1039/c2gc35152h.
[54] Fogassy G, Thegarid N, Schuurman Y, Mirodatos C. From biomass to bio-gasoline by FCC co-processing: Effect of feed composition and catalyst structure on product quality. Energy Environ Sci 2011;4:5068–76. https://doi.org/10.1039/c1ee02012a.
[55] Xing T, Alvarez-Majmutov A, Gieleciak R, Chen J. Co-hydroprocessing HTL Biocrude from Waste Biomass with Bitumen-Derived Vacuum Gas Oil. Energy Fuels 2019;33:11135–44. https://doi.org/10.1021/acs.energyfuels.9b02711.
[56] Astm. ASTM E300. Standard Practice for Sampling Industrial Chemicals. ASTM Int 2017.
[57] Thommes M, Kaneko K, Neimark A V., Olivier JP, Rodriguez-Reinoso F, Rouquerol J, et al. Physisorption of gases, with special reference to the evaluation of surface area and pore size distribution (IUPAC Technical Report). Pure Appl Chem 2015;87:1051–69. 10.1515/pac-2014-1117.
[58] Astm. D5154–10. Standard Test Method for Determining Activity and Selectivity of Fluid Catalytic Cracking (FCC) Catalysts by Microactivity Test (MAT). ASTM Int 2010:1–8.
[59] Astm. ASTM D3907–03, Standard Test Method for Testing Fluid Catalytic Cracking (FCC) Catalysts by Microactivity Test (MAT). ASTM Int 2008:1–6.
[60] Santillan-Jimenez E, Pace R, Morgan T, Behnke C, Sajkowski DJ, Lappas A, et al. Co-processing of hydrothermal liquefaction algal bio-oil and petroleum feedstock to fuel-like hydrocarbons via fluid catalytic cracking. Fuel Process Technol 2019;188:164–71.
[61] Synergistic Effect. (n.d.). AlleydogCom's Online Gloss 2022.
[62] Roell KR, Reif DM, Motsinger-Reif AA. An introduction to terminology and methodology of chemical synergy-perspectives from across disciplines. Front Pharmacol 2017;8:1–11. https://doi.org/10.3389/fphar.2017.00158.